Applied Catalysis B: Environmental 129 (2013) 287–293

Contents lists available at SciVerse ScienceDirect

Applied Catalysis B: Environmental

journal homepage: www.elsevier.com/locate/apcatb

Au/ZrO_2: an efficient and reusable catalyst for the oxidative esterification of renewable furfural

M. Signoretto[a,*], F. Menegazzo[a], L. Contessotto[a], F. Pinna[a], M. Manzoli[b], F. Boccuzzi[b]

[a] Department of Molecular Sciences and Nanosystems, Ca' Foscari University Venice and Consortium INSTM UdR Ve, Dorsoduro 2137, 30123 Venice, Italy
[b] Department of Chemistry, University of Turin, and NIS Centre of Excellence, via P. Giuria 7, 10125 Torino, Italy

ARTICLE INFO

Article history:
Received 22 June 2012
Received in revised form
17 September 2012
Accepted 21 September 2012
Available online 27 September 2012

Keywords:
Gold catalyst
Furfural
Oxidation
Biomass esterification
Zirconia

ABSTRACT

Highly dispersed gold based catalysts supported on zirconia were employed in the oxidative esterification of furfural by an efficient and sustainable process. Au/ZrO_2 catalysts were calcined at different temperatures in order to modulate gold nanosize. A detailed characterization was carried out for the sake of ascertaining if micro structural changes occurred, and the size issue was discussed. Catalysts stability and recycling were investigated too, and the opportunity of reusability by thermal oxidation at a proper temperature was successfully proved.

1. Introduction

The world needs to find new ways for generating energy and platform chemicals, doing so in an economically viable fashion while limiting environmental damage. Biomass can be considered [1] a renewable resource because it can be replenished over a relatively short timescale and it is essentially limitless in supply. In particular, ligno-cellulosic materials (e.g. wood, straw, energy crops) present a good opportunity since they avoid competition with the food sector and often do not requires as much as land and fertilisers to grow. The supply of agricultural wastes, wood industry and forest wastes looks especially promising. So, the development of ligno-cellulosic bio refineries is a strategic target, but it requires the development of new methodologies and synthesis, since they are a complex and highly integrated system. As a matter of fact, the sustainability of bio refineries derives from their ability of exploiting every product, as actually occurs in the oil refineries. In the general framework, the upgrading and valorization of C5 fraction represents a specific relevant issue. Indeed, for this fraction (xylose) there are no well developed process yet. Furfural (2-FA) can be obtained from xyloses by dehydration in acidic media and it can be used in soil chemistry and as a building block in the production of Lycra®, etc. Nevertheless, additional transformations of furfural are highly desired, that is to find new pathways for converting 2-FA to items which could be integrated into the bio refinery product chain. Among these, the synthesis of alkyl furoates (in particular methyl- or ethyl-derivatives) can open very interesting perspectives for the use of xyloses. Alkyl furoates find applications as flavor and fragrance component in the fine chemical industry.

Up to now, the upgrade of 2-FA has been little investigated in the literature [2,3]. Traditionally, the furoate ester is prepared by oxidizing furfural with potassium permanganate, preferably using acetone as solvent, and reacting the furoic acid so formed with methyl or ethyl alcohol, in the presence of sulfuric acid. The use of this substance affects a considerable environmental impact. Recently, it has been shown [2] that furfural can be converted into methyl furoate by an oxidative esterification in the presence of a base ($NaCH_3O$) in CH_3OH under mild conditions on a Au/TiO_2 reference catalyst purchased by the World Gold Council (WGC). However, in order to be applied in a large scale production, this process must be optimized, starting from the composition and the microstructure of the catalyst. Corma and co-workers have recently reported [3] a base-free synthesis of methyl furoate on a Au/CeO_2 catalyst, but increasing both temperature and pressure conditions with respect the activity test of Christensen and co-workers [2]. As a matter of fact, catalysis by gold nanoparticles is a topic of current interest, as proved by the exponential growth of the papers on this subject [4,5].

ZrO_2 has been found to be a very suitable support for gold [6–8], and we have lately focused our attention on Au/ZrO_2 samples [9,10]

* Corresponding author. Tel.: +39 041 234 8650; fax: +39 041 234 8517.
E-mail address: miky@unive.it (M. Signoretto).

0926-3373/$ – see front matter © 2012 Elsevier B.V. All rights reserved.
http://dx.doi.org/10.1016/j.apcatb.2012.09.035

for the LT-WGSR. Very recently, we have applied such highly dispersed catalysts to the esterification of furfural. We have found [11] excellent catalytic performances of a Au/ZrO_2 sample in comparison to the Au/TiO_2 catalyst provided by the World Gold Council. The noticeable differences observed between the two samples can be ascribed [11] to the presence on the Au/ZrO_2 catalyst of highly dispersed Au clusters able to produce atomic oxygen by reaction with the oxygen molecule. The choice of zirconia as support is due to its intrinsic chemical and physical characteristics that can be adjusted by choosing different precursors and synthesis conditions. Moreover, the addition of dopants, in particular sulfates, increases surface acidity, retards crystallization and enhances the surface area [12]. We have recently demonstrated [13] that sulfates addition to zirconia means a twofold advantage: (i) higher surface area; (ii) higher gold dispersion due to the positive role of SO_4^{2-} groups that address the deposition of Au in the form of highly dispersed non metallic gold clusters in close contact with the support. However, no sulfates are present in the final catalysts anymore, due to the detachment of sulfate groups during the deposition-precipitation. So, as already discussed in depth [9,10], sulfates do not behave as promoters of the gold active phase in the final samples, but they only act as structural promoters of the support. For this reason we have named the catalysts object of the present paper only as Au/ZrO_2 samples.

In the present work we show a detailed and comprehensive investigation on the role of the calcination temperature of Au/ZrO_2 samples on gold dispersion and consequently on the catalytic properties in the oxidative esterification of furfural. In particular, we have studied the reaction without the addition of $NaCH_3O$, that would make the process less green and more expensive [3]. The main part of the research highlights in depth all the sample's deactivation reasons in order to assess the possibility of catalyst's recycling. The final goal of the present paper is therefore to obtain an active, selective and recyclable catalytic system for the exploitation of renewable furfural.

2. Experimental

2.1. Catalyst preparation

$Zr(OH)_4$ was prepared by precipitation from $ZrOCl_2{\cdot}8H_2O$ at constant pH 8.6, aged for 20 h at 90 °C [13], washed with warm water free of chloride ($AgNO_3$ test), dried at 110 °C overnight. The hydroxide was sulfated with $(NH_4)_2SO_4$ (Merck) by incipient wetness impregnation in order to obtain a 2 wt% amount of sulfates on the final support. Sulfated zirconium hydroxide was then calcined in air (30 mL/min STP) at 650 °C for 3 h. 1.5 wt% of gold was added by deposition-precipitation (dp) at pH 8.6: the oxide support (5 g) was suspended in 200 mL of aqueous solution of $HAuCl_4{\cdot}3H_2O$ for 3 h and the pH was controlled by the addition of NaOH (0.5 M).

After filtration the sample was dried at 35 °C overnight and finally calcined in air for 1 h at different temperatures (150 °C, 300 °C, 500 °C, 600 °C, 650 °C). Au/ZrO_2 samples were denoted as AZ150, AZ300, AZ500, AZ600, AZ650 respectively.

Oxidative treatments of the exhausted catalysts were carried out with a temperature rate of 2 °C/min from 25 °C to the proper temperature in a $5\%O_2$/He flow (40 mL/min).

2.2. Methods

The sulfate content of all samples was determined by ion chromatography (IC). Sulfate concentration was calculated as the average of two independent analyses, each including two chromatographic determinations.

The gold amount was determined by atomic adsorption spectroscopy. Dried samples (typically 100 mg) were dispersed in water acidified with HF and aqua regia and disaggregated by microwaves.

CO pulse chemisorption measurements were performed at −116 °C in a lab-made equipment. Before the analysis the following pretreatment was applied: the sample (200 mg) was reduced in a H_2 flow (40 mL/min) at 150 °C for 60 min, cooled in H_2 to room temperature, purged in He flow and finally hydrated at room temperature. The hydration treatment was performed by contacting the sample with a He flow (10 mL/min) saturated with a proper amount of water. The sample was then cooled in He flow to the temperature chosen for CO chemisorption (−116 °C) [10].

FTIR spectra were taken on a PerkinElmer 1760 spectrometer (equipped with a MCT detector) with the samples in self-supporting pellets introduced in a cell allowing thermal treatments in controlled atmospheres and spectrum scanning at controlled temperatures. The obtained integrated areas were normalized to the Au content of each sample. Before the measurements, the samples were submitted to an oxidative pretreatment and a reductive one. In particular, the oxidative treatment included heating from room temperature (r.t.) to 150 °C under outgassing; followed by an inlet of O_2 (20 mbar) and heating up to 180 °C; the O_2 was changed three times (20 mbar for 10 min each one) at such temperature. The sample was then cooled down to r.t. in oxygen and finally outgassed at the same temperature. The reductive treatment was carried out (after oxidation) by heating from r.t. up to 150 °C in H_2 (10 mbar), keeping that temperature for 10 min. After that, the sample was cooled to r.t. under outgassing. The samples will be denoted as "as prepared" after this activation procedure.

HRTEM analysis was performed on all catalysts using a Jeol 3010 EX electron microscope (300 kV) equipped with a side entry stage and a LaB_6 filament. The powdered samples were ultrasonically dispersed in isopropyl alcohol and the obtained suspension was deposited on a copper grid, coated with a porous carbon film. The mean particle diameter and size distribution were obtained by counting a statistically significative number of gold particles (at least 300).

TPO measurements were carried out in a lab-made equipment: samples (100 mg) were heated with a temperature rate of 10 °C/min from 25 °C to 600 °C in a $5\%O_2$/He flow (40 mL/min). The effluent gases were analyzed by a TCD detector and by a Genesys 422 quadrupole mass analyzer (QMS).

2.3. Catalytic activity measurement

Furfural oxidative esterification with oxygen and methanol was investigated at 120 °C, without $NaCH_3O$ addition, using a mechanical stirred autoclave fitted with an external jacket. Catalyst (100 mg), furfural (300 μL) and n-octane (150 μL), used as internal standard, were added to the solvent (150 mL of methanol)(molar ratio Au/furfural/MeOH = $1/5 \times 10^3/5 \times 10^6$). The reactor was charged with oxygen (6 bar) and stirred at 1000 rpm. The progress of the reaction was determined after 3 h (if not specified otherwise) by gas-chromatographic analysis of the converted mixture (capillary column HP-5, FID detector). Preliminary experiments showed that the system works in a strictly kinetic regime.

3. Results and discussion

3.1. The role of gold nanosize on the oxidative esterification of furfural

Catalysts have been calcined at different temperatures in order to modulate gold nanosize and investigate its role in the oxidative esterification of furfural to methyl furoate. Such reaction has been

Table 1
Gold content and activity data of the samples.

Sample	Au found (wt%)	Conversion (%)	Methyl furoate selectivity (%)	Chemisorptions data (mol_{CO}/mol_{Au})
AZ150	1.5	99	94	0.24
AZ300	1.5	98	94	0.23
AZ500	1.5	100	98	0.03
AZ600	1.5	57	76	0.01
AZ650	1.5	24	60	0.01

carried out in methanol without the addition of $NaCH_3O$, that would make the process less green and more expensive [3].

A part from the methyl furoate, the only by-product that was found is the acetal derivate, as revealed by mass spectroscopy. Under the experimental conditions, the moles of furfural, methyl furoate and acetal perfectly close the mass balance, so we can exclude the formation of other by-products.

In Table 1 the conversions and the methyl furoate selectivities after 3 h of reaction for the five catalysts are reported. All samples calcined until 500 °C show very good catalytic performances for both activity and selectivity. On the contrary, conversions and selectivities obtained for the AZ600 and AZ650 samples are noticeably lower.

A detailed characterization has been carried out in order to verify if micro structural changes occurred on the Au/ZrO_2 catalyst calcined at different temperatures. HRTEM analysis revealed a very high Au dispersion, the results are shown in Fig. 1 (where the images are reported) and Fig. 2 in which the particle size distributions are presented. Only very small roundish Au particles and clusters with average size of 1.8 ± 0.2 nm have been observed in the AZ150 catalyst (Fig. 1, section a). The particle size distribution related to this sample is quite narrow and symmetric (see section a of Fig. 2), indicating that the gold nanoparticles are very small, having homogeneous size mainly between 1 and 2 nm. Nevertheless, very small gold species with size below 1 nm (0.7 nm), i.e. clusters, have been detected, too. Moreover, the presence of gold species even smaller cannot be excluded, since their size is below the detection limit of the microscope.

Both gold size and morphology are unchanged after calcination treatment at 300 °C (section b of Fig. 1), being the average diameter $d_m = 1.9 \pm 0.4$ nm. The shape of the particle size distribution is similar to that related to AZ150, but slightly shifted toward higher sizes. Nevertheless, the data evidence that also on AZ300 the gold dispersion is very high (very small particles and clusters are present). On the contrary, the gold nanoparticles appear bigger (section c of Fig. 1) when the calcination temperature is raised up to 500 °C and the obtained average size is $d_m = 2.7 \pm 0.7$ nm. The particle size distribution reported in section c of Fig. 2 well describes the changes occurred on the sample during the calcination at 500 °C.

In fact, the shape of the distribution results markedly enlarged if compared to those related to AZ150 and AZ300 and gold particles with size ranging from 1.5 to 4.5 nm have been observed. However, a large fraction of particles still remains very small, having size below 2.5 nm, indicating that the thermal treatment at high temperature did not compromise totally the gold dispersion and that very small particles and, possibly, clusters coexist together with larger particles. As a matter of fact, both conversion and selectivity to methylfuroate, that are reported in Table 1, are maintained.

The calcination at 600 °C has a dramatic effect on the size of gold: big particles with average diameter $d_m = 4.9 \pm 1.3$ nm have been observed in conjunction with a small increase of zirconia particles size (section d of Fig. 1), while the gold particle size distribution extends in the size range between 3 and 9 nm, with the disappearance of small particles and clusters. These features are accompanied

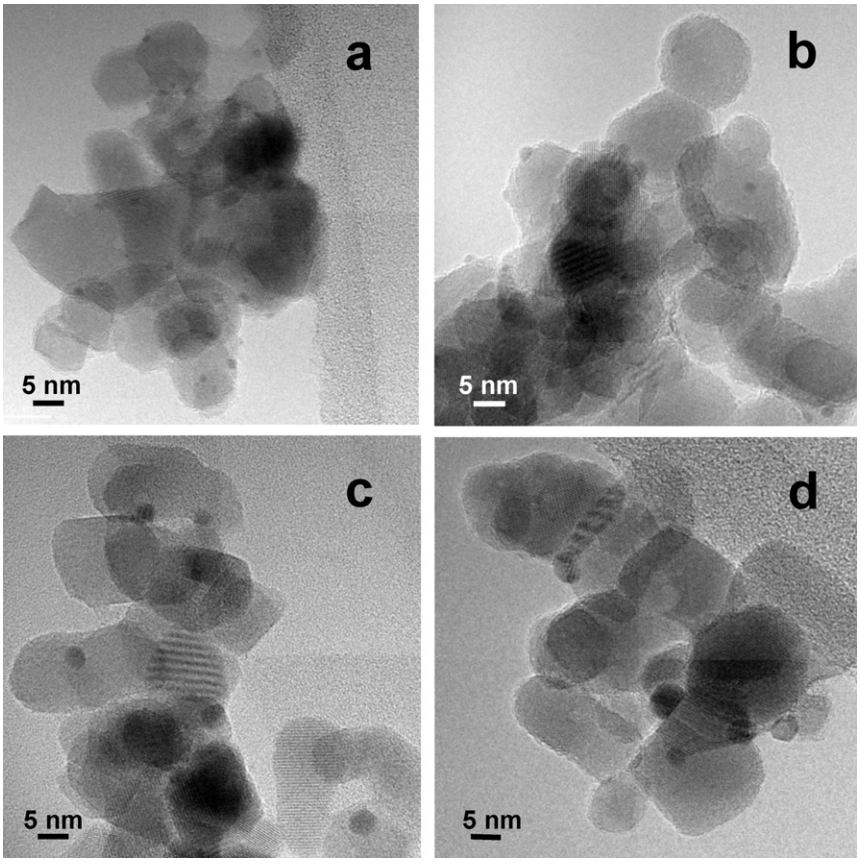

Fig. 1. HRTEM images of AZ150 (section a), AZ300 (section b), AZ500 (section c) and AZ600 (section d). Instrumental magnification: 300,000×.

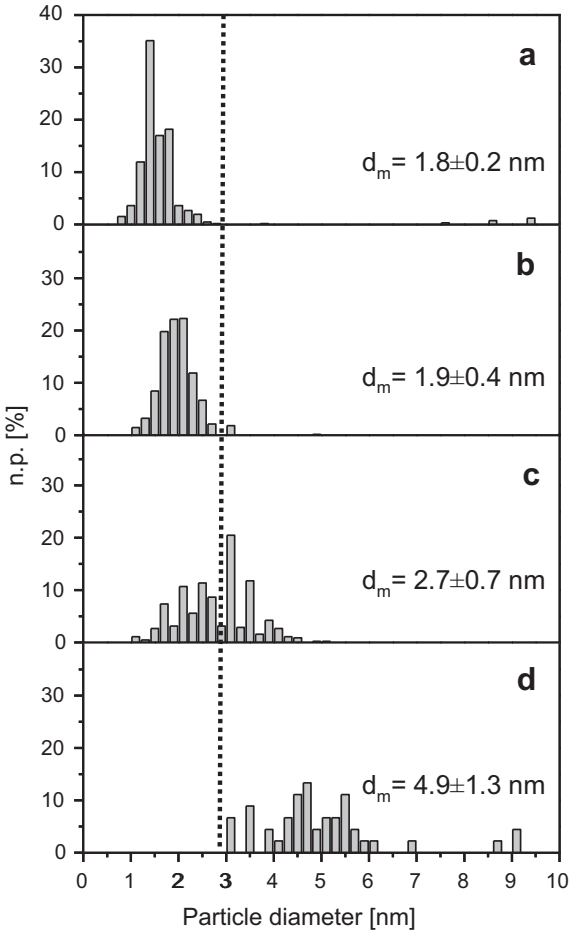

Fig. 2. Gold particle size distribution of AZ150 (section a), AZ300 (section b), AZ500 (section c) and AZ600 (section d). Dashed line evidences the limiting size for active and selective gold nanoparticles.

by a drastic decrease in productivity and selectivity of the catalyst, as reported in Table 1. However, the HRTEM findings alone do not allow a full interpretation of the catalytic results. For this reason, FTIR spectroscopy of adsorbed CO has been used to obtain additional information on the nature of the exposed gold sites on the different samples. The comparison between AZ300 and AZ500 is shown in Fig. 3, where the CO adsorption spectra collected at r.t.

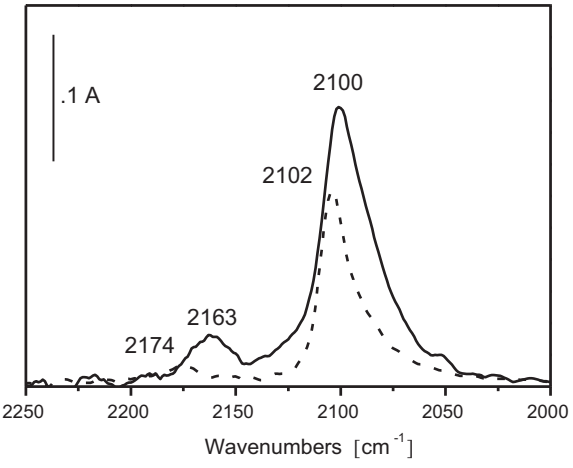

Fig. 3. CO adsorbed at r.t on the as prepared AZ300 (solid curve) and AZ500 (dashed curve) catalysts.

Table 2
Catalytic performances of the samples at different reaction times.

Sample	Conversion (%)	Methyl furoate selectivity(%)	Time (min)
AZ150	25	94	15
AZ150	47	93	40
AZ150	70	94	90
AZ300	26	94	15
AZ300	49	93	40
AZ300	73	94	90
AZ500	37	96	15
AZ500	63	96	40
AZ500	96	97	90

are reported in the carbonylic region after being normalized on the gold content of each pellet. CO adsorption at r.t. on the as prepared AZ300 sample (solid curve) produces a quite intense and symmetric band at 2100 cm^{-1}, that is assigned to CO on less coordinated Au^0 sites of gold clusters and small nanoparticles [9], and a weak band a 2163 cm^{-1}, due to CO on Zr^{4+} sites of the support [14]. On the contrary, CO adsorption at room temperature on as prepared AZ500 (dashed curve) produces a band at 2102 cm^{-1}, that is quite different in shape and sensibly less intense than that related to AZ300. In fact, this band is asymmetric with an evident tail at lower frequencies. The component at 2102 cm^{-1} is related to CO on Au^0 sites exposed at the surface of nanoparticles [15], while the component at lower frequencies is due to CO on less coordinated Au^0 sites of clusters and small nanoparticles [9]. Finally, the very weak band a 2174 cm^{-1} assigned to CO on less coordinated Zr^{4+} sites of the support [17]. Hence, the spectroscopic findings evidence the presence of gold clusters, not only on AZ300, but also on AZ500, where HRTEM observations were ambiguous.

Nevertheless, all catalysts calcined below 500 °C present almost complete conversion and selectivity. In order to identify the best sample, we have performed different catalytic tests by varying the time of reaction (Table 2). For all the catalysts selectivity is constant for the duration of the tests. On the contrary, conversions increase with reaction time, but in this case the AZ500 catalyst present always higher values than AZ150 and AZ300 catalysts. A possible explanation can be ascribed to the fact that on AZ150 and AZ300 very small clusters, (with size well below 0.7 nm and not detectable by HRTEM) are present, due to the low calcination temperature of the catalysts during preparation. The interaction between these smallest clusters and atomic oxygen could be stronger than on the biggest ones, observed on AZ500. These data clearly show that it is very important to make the right choice for the calcination temperature, in order to suitably modulate gold nanosize.

Fig. 4 reports the catalytic performances of the Au/ZrO_2 samples vs CO chemisorption data. In particular, TOF number calculated after 15 min of reaction are reported in relationship

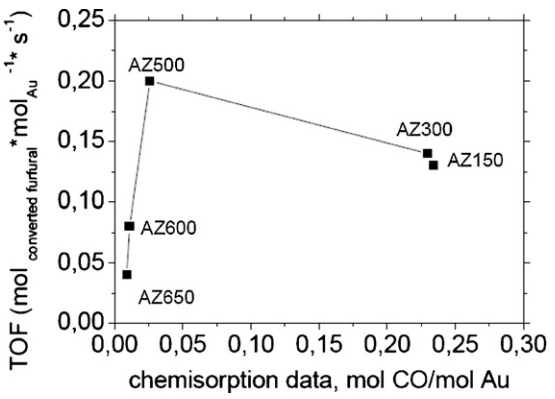

Fig. 4. Catalytic performances of the Au/ZrO_2 samples vs chemisorption results.

with CO chemisorptions data. AZ500 is clearly more active than AZ600 and AZ650, according to the following trend: AZ500 ≥ AZ300 ≈ AZ150 ≫ AZ600 > AZ650. The CO chemisorption is reported as mol_{CO}/mol_{Au} ratio, being an indication of the number of less coordinated gold sites able to absorb CO. These sites can be also involved in oxygen activation and the above ratio allows to compare directly all samples, since it refers to the number of moles of Au in each sample. As a consequence, CO chemisorption gives also a measure of gold dispersion [10]. In fact, a high mol_{CO}/mol_{Au} ratio can be related to the presence of clusters, exposing a high number of uncoordinated sites, while the Au/ZrO_2 catalysts undergone to thermal treatment at 600 °C and 650 °C have a low mol_{CO}/mol_{Au} value, meaning that larger gold particles are present on these catalysts. AZ150 and AZ300 have almost the same high chemisorption capability that indicates the presence of Au clusters, while in the case of AZ500 the mol_{CO}/mol_{Au} ratio is lower and it can be related to the presence of both small Au nanoparticles and clusters.

These findings well agree with the results of the combined FTIR and HRTEM analyses. Fig. 4 evidences again that a drastic decrease of TOF occurs on samples calcined at a temperature higher than 500 °C. In fact, at $T > 500$ °C, all clusters coalesce to form nanoparticles, as indicated by CO chemisorption and HRTEM measurements. Therefore, we are able to define a limiting upper size for active gold, that is about 3 nm (2.5 nm). These findings are in good agreement with data obtained for the CO oxidation reaction by Goodman and co-workers [16] on Au/TiO_2, Au species with size of 3.5 nm exhibiting the maximum reactivity. The limiting size appeared related to an intrinsic modification of the properties of Au clusters with respect to nanoparticles. In fact, Au clusters are able to activate molecular oxygen producing atomic O species, that render the catalyst more active for furfural esterification reaction [11].

3.2. Investigation on stability and reusability of the catalysts

The nature of catalyst deactivation and the possibility of regaining lost catalytic activity either during the operation of the reaction or in a separate regeneration step, are important factors that determine process options [17]. So, we have investigated the stability and the reusability of our most active sample, that is of the AZ500 catalyst (AZ). To shed light on this point, first of all experiments were performed with sample after the first catalytic run: the solid was filtered off, washed with methanol and dried at 110 °C overnight (AZd). However, this procedure is not sufficient to restore starting performances, as reported in Fig. 5. In fact, after this treatment conversion and particularly selectivity are very low. It is known that there are many reasons for the loss of activity during a process are poisoning or reaction inhibition by impurities in the feed or by reaction by-products, deposition of polymeric material including coke as a result of side or consecutive reactions, and loss of catalyst dispersion by sintering of small particles of the active material. In addition, catalysts may become deactivated by loss of active components by leaching, or by changes in their porous texture [18]. So, we decided to examine the reasons of samples deactivation in the oxidative esterification of furfural more in depth: in particular we examined metal leaching, gold sintering, fouling of the active sites.

3.3. Metal leaching

Working in solvent medium, metal leaching cannot, in principle, be excluded and the heterogeneity of the catalytic reaction may be questionable. Therefore, we investigated gold leaching through chemical analysis by atomic absorption of the disintegrated exhausted samples. The as prepared samples have 1.5 wt% of gold, and catalysts that have been discharged after 3 h of reaction

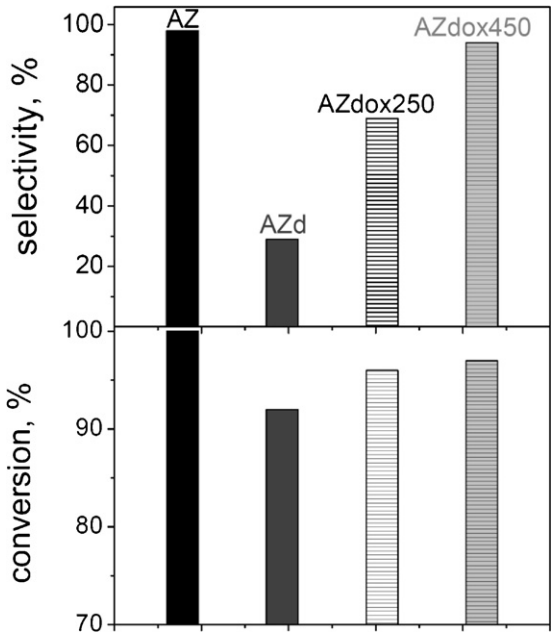

Fig. 5. Conversion and selectivity of the AZ500 catalyst: 1st run (as prepared: AZ), 2nd run after drying (AZd), 2nd run after oxidation at 250 °C (AZdox250) and 2nd run after oxidation at 450 °C (AZdox450).

present the same metal content. As a consequence, we can rule out metal leaching as deactivation cause of our samples.

3.4. Metal sintering

Another reason for the selectivity decrease of Au/ZrO_2 catalysts could be associated with the sintering of gold clusters during the reaction. Therefore, the increase in size of the Au nanoparticles was also investigated. In fact, as previously discussed, it is an opportune gold dispersion, i.e. below 2.5 nm, which determines the high selectivity of Au based catalysts. In section a of Fig. 6 the HRTEM micrograph of the AZ500 sample after the reaction in autoclave and drying (AZd) is reported. As shown, it presents the same metal dispersion of the as prepared AZ500 catalyst (see sections c of Fig. 1 and Fig. 2). From these findings, gold sintering problems throughout the reaction time can be excluded.

3.5. Fouling of the active sites

In order to investigate more in depth the exhausted AZ500 sample, a FTIR analysis of adsorbed CO on the AZ500 sample submitted to different pretreatments has been performed and the results are shown in Fig. 7, section a. CO adsorption at room temperature on as prepared AZ500 has been already commented previously. However, the spectrum has been reported also here for the sake of clarity (solid black curve). In summary, FTIR evidenced less coordinated Au^0 sites of clusters and small nanoparticles [9] and Zr^{4+} sites of the support [14]. CO adsorption has been carried out at r.t., so the last absorption band is not indicative of the abundance of the support sites. In fact, to have information about these sites, it is necessary to look at the FTIR spectrum of the sample in the whole spectroscopic range before CO inlet (solid black curve in section b of Fig. 7), where weak bands related to carbonate-like species are observed at 1570–1330 cm^{-1}, evidencing that the surface of the catalyst is quite clean. After reaction and drying (solid gray curve in section a), the band due to CO on gold sites is noticeably decreased in intensity and shifted up at 2121 cm^{-1}. The observed shift (from 2098 cm^{-1} to 2121 cm^{-1}) is due to the oxidation of the gold sites, exposed

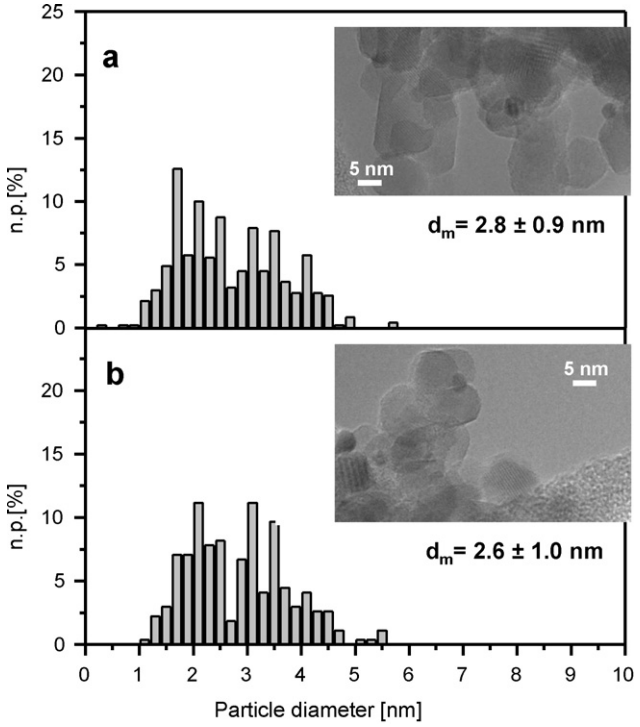

Fig. 6. Particle size distribution of the AZ500 sample after the 1st catalytic run and drying (AZd, section a) and after the 1st catalytic run and oxidation at 450 °C (AZdox450, section b). Insets: HRTEM micrographs of the AZ500 sample after the reported experimental conditions. Instrumental magnification: 300,000×.

at the surface of the clusters, occurred during and after the reaction. It is common knowledge that highly dispersed gold with size below 2 nm is able to bind the oxygen atom. At the same time, the drop of intensity is related to a partial coverage of the sites by

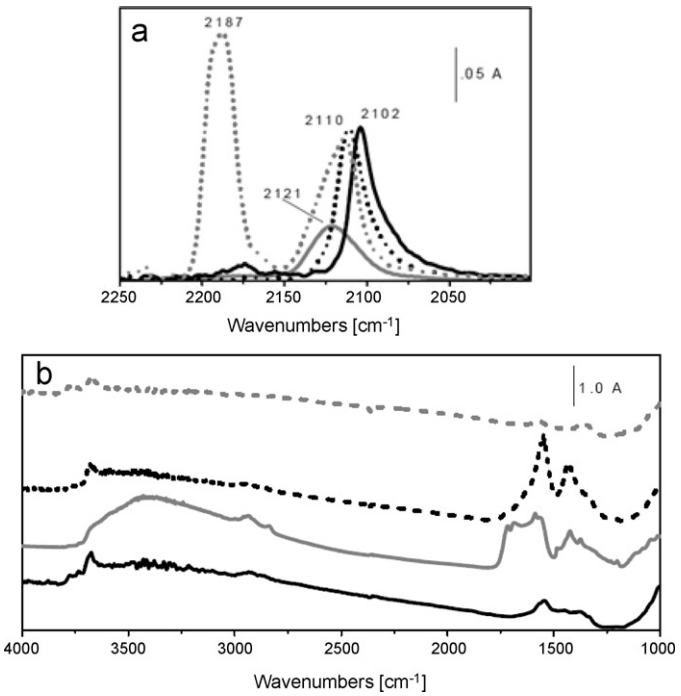

Fig. 7. Section a: CO adsorbed at r.t on the AZ500 catalyst: as prepared (AZ, solid black curve), after reaction and drying (AZd, solid gray curve), after reaction and oxidation at 250 °C (AZdox250, dashed black curve) and after reaction and oxidation at 450 °C (AZdox450, dashed gray curve). Section b: spectra of the same samples before the CO inlet in the whole spectroscopic range.

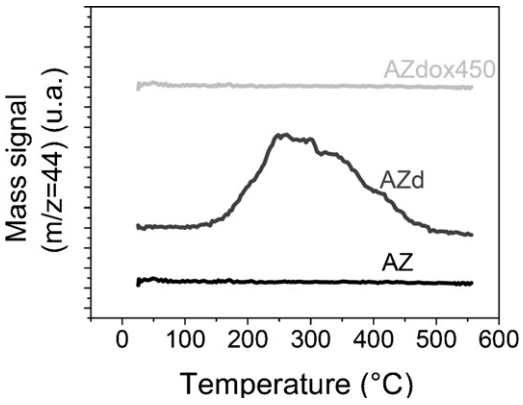

Fig. 8. TPO of the AZ500 catalyst: as prepared (AZ), after the 1st run and drying (AZd), after the 1st run and oxidation at 450 °C (AZdox450).

species formed during the reaction. Such feature is confirmed by the presence of strong bands in the 1150–1750 cm^{-1} range, due to not definite carbonate-like and carbon-containing species are well evident (see section b, solid gray curve).

The comparison between the as prepared AZ500 sample (AZ, solid black curves) and the same sample after reaction in autoclave and drying (AZd, solid gray curves) clearly indicates that both support and metal sites have not the same adsorption capability after the 1st catalytic run. This feature could be ascribed to the possible presence of reaction intermediates and/or products that are able to block the sites inhibiting the adsorption. Therefore, as revealed by FTIR analysis, a third reason for catalysts deactivation can be due to blocking of gold active sites by deposition of poisons or rather to reaction inhibition by reaction substrate, products or by-products, or even to deposition of polymeric material as a result of side or consecutive reactions.

In order to verify the presence of carbon residue, the catalyst was subjected to temperature programmed oxidation (TPO), measurements in which effluent gases were analyzed both by a TCD detector and a quadrupole mass analyzer. The results are presented in Fig. 8. The profile of the as prepared catalyst does not present CO_2 evolution, indicating the absence of organic residues in the material. On the contrary, after 3 h of oxidative esterification of furfural, we note in the TPO spectra the presence of one broad band that starts at about 150 °C and close at 500 °C. The band is due to CO_2 evolution, as confirmed by mass spectroscopy, that is probably due to decomposition of organic species in close interaction with gold active sites and with the oxide material respectively. As a result, we decided to heat the catalyst in oxygen atmosphere, in order to eliminate organic poisons. First of all, the sample was regenerated at 250 °C (AZdox250). The results of the catalytic tests are reported in Fig. 5. Conversion is slightly increased with the thermal regeneration at 250 °C. Moreover, it is possible to partially raise the selectivity (69%) after the thermal regeneration at 250 °C with respect to the only dried AZd sample (29%), but not to restore the initial one (98%).

At the same time, a detailed FTIR analysis has been carried out on this sample and the result is reported in Fig. 7 (dashed black curve). CO adsorption at r.t. shows that the band related to gold sites is totally restored in intensity and slightly shifted toward higher frequencies if compared to the initial band observed on the as prepared catalyst (solid black curve). The shift is due to an oxidation of the gold sites during the thermal treatment in oxygen atmosphere. On the contrary, looking at the spectrum of the sample before the CO inlet (dashed black curve in section b of Fig. 7), the presence of the organic residue covering the Zr^{4+} sites is confirmed by bands at 1200–1750 cm^{-1}, indicating that the organic residue can be removed by treatment at 250 °C from Au, but not completely from the support.

These results seem to suggest that the Au/ZrO_2 catalytic activity can be associated not only with the size of the gold species, or with the amount of low-coordinated sites, but that also the support plays a key role in the reaction. So, in order to completely remove the carbon residue from both gold active sites and support, the catalyst has been regenerated at 450 °C (AZdox450).

We have therefore performed catalytic reaction after the oxidative treatments at 450 °C, and the results are reported in Fig. 5. As shown, after this thermal regeneration it is possible to completely restore the initial conversion and almost fully the selectivity.

The TPO profile of the AZdox450 sample (Fig. 8) shows the absence of CO_2 evolution, meaning the complete elimination of carbon species on the material. At the same time, FTIR results well evidenced that by treatment at 450 °C the organic residue is effectively removed from both Au and support sites. More in detail, a band at 2110 cm^{-1} with a marked shoulder at higher frequencies is observed (dashed gray curve, section a of Fig. 7). Again, the shift and the presence of a component at about 2130 cm^{-1} are an indication that an oxidation of the gold sites is occurred during the cleaning procedure in oxygen atmosphere, giving further evidence of the presence of gold clusters also on AZ500. Moreover, an intense absorption band at 2182 cm^{-1}, assigned to more uncoordinated Zr^{4+} sites of the support [14] is observed: at the same time, no absorption bands in the carbonate-like region have been detected (see dashed gray curve in section b of Fig. 6).

From the foregoing it may be concluded that the change in conversion and selectivity in the second run of the catalyst under consideration is probably due to its tendency to adsorb organic species in the reaction ambient, and their accumulation during the 3 h of reaction. The deactivation in this case is reversible and after heating in oxygen atmosphere the catalyst surface is liberated by evolution of carbon dioxide. However the regeneration treatment at 450 °C could provoke a change in the gold dispersion. This is an important point since, as previously discussed, it is the high gold dispersion which determine the high selectivity of Au based catalysts. In order to have a correct determination by CO chemisorption analyses [10,15], we have performed measurements on the regenerated sample, that is in the catalyst with a clean surface, able to absorb the probe molecules. In fact the sample discharged by the reactor, as shown by TPO curve, is covered with organic species and cannot chemisorb CO. We have found for the AZdox450 sample a mol_{CO}/mol_{Au} ratio of 0.025, to be compared with the value 0.026 of the as prepared sample. Therefore, on chemisorption basis, we can exclude sintering of gold cluster in the regenerated sample, that could occur either in the reaction condition or in the oxidative treatment of regeneration.

Chemisorption results are in complete agreement with the HRTEM data, as shown in section b of Fig. 6, where the particle size distribution of the AZdox450 sample is reported. If compared to the particle size distributions related to the as prepared (see Fig. 2) and to the catalyst after reaction (reported in section a of Fig. 6), the particle size distribution is practically unchanged and gives an average diameter of $d_m = 2.6 \pm 1.0$ nm. The presence of a proper gold size is observed also in the regenerated catalyst.

In summary, after thermal regeneration at 450 °C it is possible to completely restore the initial conversion and almost fully the selectivity. This is due to the complete absence of organic residue from both gold and zirconia, as discussed by TPO and FTIR, and to the presence of the proper gold size also in the regenerated catalyst, as demonstrated by chemisorption and HRTEM analyses.

4. Conclusions

Au/ZrO_2 calcined at a proper temperature is an efficient catalyst for the oxidative esterification of furfural. In particular, the calcination at 500 °C allows to modulate gold nanosize (below 3 nm) and above all to stabilize gold clusters, that are able to dissociate oxygen.

In addition, beside the choice of the best preliminary calcination temperature, a very important point is the stability and reusability of the catalyst. In particular, an oxidation treatment at the proper temperature of the exhausted catalyst allows to almost completely recover catalytic performances, because it allows to remove the organic residue from both gold active sites and zirconia. The obtained results suggest that the support is important in the furfural esterification reaction.

The catalyst AZ500 is therefore active, selective, recyclable and proper for an industrial chemistry based on renewable resources. The furoate ester can be obtained with optimal yields by a process greener than the actual one.

Acknowledgments

We thank Mrs.Tania Fantinel for technical assistance. Financial support to this work by MIUR (Cofin 2008) is gratefully acknowledged.

References

[1] J.H. Clark, F. Deswarte, Introduction to Chemicals from Biomass, Wiley-VCH, 2008, pp. 1–3, ISBN: 978-0-470-05805-3, © 2008 John Wiley & Sons, Ltd.
[2] E. Taaring, I.S. Nielsen, K. Egeblad, R. Madsen, C.H. Christensen, ChemSusChem 1 (2008) 75–78.
[3] O. Casanova, S. Iborra, A. Corma, Journal of Catalysis 265 (2009) 109–116.
[4] A. Corma, H. Garcia, Chemical Society Reviews 37 (2008) 2096–2126.
[5] R. Meyer, C. Lemire, Sh.K. Shaikhutdinov, H.-J. Freund, Gold Bulletin 37 (2004) 72.
[6] V. Idakiev, T. Tabakova, A. Naydenov, Z.-Y. Yuan, B.-L. Su, Applied Catalysis B 63 (2006) 178–186.
[7] A. Kuperman, M. Moir, WO 2005 005032 (2005).
[8] M. Boaro, M. Vicario, J. Llorca, C. de Leitenburg, G. Dolcetti, A. Trovarelli, Applied Catalysis B 88 (2009) 272–282.
[9] F. Menegazzo, F. Pinna, M. Signoretto, V. Trevisan, F. Boccuzzi, A. Chiorino, M. Manzoli, ChemSusChem 1 (2008) 320–326.
[10] F. Menegazzo, F. Pinna, M. Signoretto, V. Trevisan, F. Boccuzzi, A. Chiorino, M. Manzoli, Applied Catalysis A 356 (2009) 31–35.
[11] F. Pinna, A. Olivo, V. Trevisan, F. Menegazzo, M. Signoretto, M. Manzoli, F. Boccuzzi, Catalysis Today, http://dx.doi.org/10.1016/j.cattod.2012.01.033
[12] X. Song, A. Sayari, Catalysis Reviews: Science and Engineering 38 (1996) 329–412.
[13] M. Manzoli, F. Boccuzzi, V. Trevisan, F. Menegazzo, M. Signoretto, F. Pinna, Applied Catalysis B 96 (2010) 28–33.
[14] C. Morterra, V. Bolis, B. Fubini, L. Orio, T.B. Williams, Surface Science 251–252 (1991) 540–545.
[15] F. Menegazzo, M. Manzoli, A. Chiorino, F. Boccuzzi, T. Tabakova, M. Signoretto, F. Pinna, N. Pernicone, Journal of Catalysis 237 (2006) 431–434.
[16] M. Valden, X. Lai, D.W. Goodman, Science 281 (1998) 1647–1650.
[17] S.T. Sie, Applied Catalysis A 212 (2001) 129–151.
[18] S. Brunauer, P.H. Emmett, E. Teller, Journal of the American Chemical Society 60 (1938) 309–319.